ACADEMIC PRESS

Available online at www.sciencedirect.com
SCIENCE DIRECT®

Journal of Catalysis 216 (2003) 324–332

JOURNAL OF CATALYSIS

www.elsevier.com/locate/jcat

Toward a molecular description of heterogeneous catalysis: transition metal ions in zeolites

Annick Goursot,* Bernard Coq, and François Fajula

Laboratoire de Matériaux Catalytiques et Catalyse en Chimie Organique, UMR CNRS-ENSCM 5618, ENSCM, 8 rue de l'Ecole Normale, 34296 Montpellier cedex 5, France

Received 24 July 2002; revised 20 September 2002; accepted 2 October 2002

Abstract

Quantum mechanical modeling of the properties of transition metal ions (TMI) in zeolites gives a picture of the material which corresponds to that of a large organometallic system in which the zeolite framework behaves as a multidentate ligand. The electron density is distributed among the whole system with highly delocalized frontier orbitals. Analyses of the electron density changes in Cu–ZSM-5 and Cu–FAU models upon adsorption and desorption of donor or acceptor ligands point to a supermolecular behavior of the whole system where the zeolite framework acts as a reservoir of electronic charge. This molecular description of TMI-zeolites provides a rational explanation of various aspects of their catalytic behavior in the decomposition and selective catalytic reduction (SCR) of nitrogen oxides, such as the nature of the rate determining step and the positive influence of protons in the SCR of NO by NH_3.

Keywords: TMI-zeolites; Decomposition of nitrogen oxides; Catalytic reduction; Quantum Mechanical calculations

1. Introduction

Description of catalytic reactions at the molecular level has been achieved for some homogeneous catalysts or in a limited number of cases for model surfaces but remains a challenge for most heterogeneous systems. Such a description would suppose a precise knowledge of the state of the working surface from both structural and electronic points of view. In spite of continuous advances in the development of in situ characterization techniques, this knowledge is still hardly accessible. The phenomena relevant to catalysis are generally concerned with a limited number of "active sites" sitting on the surface of highly dispersed solids. Crystallographically well-ordered covalent or ionic surfaces are not achievable in small crystals as a result of stability-driven recrystallization and relaxation processes. This generally hampers any realistic representation of active catalytic metal and metal oxide surfaces at the atomic scale. In that context, zeolites constitute a unique class of materials. Zeolites are stable crystalline materials in which all crystal atoms may be considered as surface atoms, at least for reactions involving small molecules. The active surface is embedded within the crystal and can be reliably modeled from the atomic coordinates and treated quantum chemically. Such a favorable situation, combined with the increase of computational power, has enabled significant advances in our understanding of the molecular aspects of catalysis at solid surfaces. A remarkable illustration of this statement is given in this account and concerns transition metal ions (TMI) in zeolites. TMI-zeolites constitute a class of active and selective catalysts for a variety of reactions, including redox transformations. They are thus gaining much interest owing to their efficiency for the decomposition and the selective reduction of nitrogen oxides.

NO_x ($NO + NO_2$) emissions are responsible for acid rain (deforestation), photochemical smog (health desease), and intensification of ground-level ozone. Besides its contribution to global warming, N_2O takes part in the depletion of the stratospheric ozone layer. There is thus a strong incentive to reduce NO_x and N_2O emitted from domestic and industrial human activities. Obviously, emissions from stationary sources of industrial processes are the easiest to control and technologies based on zeolites are currently in use [1]. In particular, TMI-zeolites are among the most efficient catalytic materials for the catalytic decomposition of NO and

* Corresponding author.
E-mail address: goursot@rhodium.enscm.fr (A. Goursot).

0021-9517/03/$ – see front matter
doi:10.1016/S0021-9517(02)00110-0

N_2O, and for the selective catalytic reduction (SCR) in the presence of oxygen of NO_x and N_2O using various types of reductants. A nonexhaustive list of review papers have dealt with this subject [2–8]. This very large body of work about nitrogen oxide removal on TMI-zeolite reveals that the most active species are isolated cations, or oxocations, of very low nuclearity. The chief function of the zeolite framework is the stabilization of these species under reaction conditions. It was well demonstrated that large TM oxide aggregates exhibit lower reactivity and selectivity. Several factors may influence the catalytic properties of TMI-zeolite for nitrogen oxide transformation: the nature of the zeolite, the amount and siting of TMI, the nuclearity of active species, the presence of cocations, and so on. Besides the classical approach of confronting the reactivity and characterization of the materials, a deeper understanding of the behavior of TMI-zeolite can be expected from quantum chemical calculations, in hope of a better prospect for designing novel catalysts with improved properties. We will give an outlook of this aspect, as it is addressed in our group.

2. The importance of quantum chemical calculations on TMI-zeolite

The understanding of catalytic reactions in zeolites necessitates a realistic description of (i) the zeolite material; (ii) the reactants; (iii) their interaction in the reaction conditions. Each of these modeling steps represents a complex study. A large number of recent papers has been devoted to step 1, focusing on the siting and stability of TMIs at various sites of the zeolite, essentially ZSM-5 [9–11], with few studies on chabazite [12], and faujasite-type structures [13–15]. Comparison with spectroscopic data, from UV–visible and EPR experiments, has allowed us to validate some models of cationic sites [14–16].

Formal Cu(II)/Cu(I) or Fe(III)/Fe(II) redox couples are currently proposed in the mechanistic explanations of NO_x or N_2O decomposition [8, and references therein]. This should not be taken literally—concentrating the reactivity into the TMI being thus the main actor of the catalysis, able to donate or receive one electron according to the need of the catalytic cycle. The concept of ionic framework–cationic partners, used for adsorption in alkali-zeolites or for acid catalysis, assuming already abstracted protons, is not realistic for TMI-zeolites.

Actually, it is well known, from organometallic chemistry, that neutral or anionic molecular ligands form bonding interactions with TMIs, the electron density being distributed among the whole system, as described within a molecular orbital (MO) picture. Moreover, according to the reaction conditions, there may be a competition between outgoing and incoming ligands. A zeolite framework can be considered as a peculiar ligand, being mono-, bi-, . . . , hexadentate, according to the site where the metal ion is located and its interaction with incoming molecules such as H_2O, NH_3, NO, etc.

The idea that TMI-zeolite catalysts behave as supermolecules including multidentate metallic sites and reactants will be presented in upcoming sections. It is based on the analysis of quantum mechanical (QM) results published in the literature for different model systems of TMI-zeolites. The comparison of these data leads to a unified interpretation of the electronic properties of these systems. The ability of the framework to accommodate cation exchanges (alkalis with protons or TMIs) and adsorption of molecules has been demonstrated by numerous experimental and theoretical studies, showing substantial changes in the geometries and vibrational properties [11,17–20]. Geometrical changes are always related with electronic changes. The electron distribution in a TMI-zeolite differs substantially from alkali systems (Section 3.2) and it also changes unambiguously upon adsorption of guest molecules on metallic sites (Section 3.3). The electron density distribution in the whole system also depends on the presence of TMI cocations (Section 4.3). We believe that all these results are indicative of supermolecular behavior.

3. Modeling TMI-zeolites

3.1. The siting of TMI

Although simple models may account for interesting trends of the reactivity of TMI-zeolites, modeling their electronic properties is a complex task, related to the double local and nonlocal nature of the zeolite ligand:

1. The local geometry in the vicinity of the transition metal ion (or oxocation) may display distortions, more pronounced for TMI^{2+} or TMI^{3+} (Cu^{2+}, Zn^{2+}, Fe^{3+}), according to the relative Al positions in the framework;
2. The TMI coordination and the positions of the nearest cocations depend on the distribution of Al in the framework, determined by the synthesis in the presence of alkali or organic cations, later exchanged with TMIs, i.e., a nonlocal influence.

Quantum mechanical studies using cluster models combined or not with a molecular mechanics (MM) description of the surroundings have been devoted to the analysis of the possible sites and coordination of Cu^+, Cu^{2+}, Zn^{2+}, and other divalent cations in ZSM-5, and Cu^{2+} or Co^{2+} in FAU. More detailed information on siting and coordination can be found in [9–11,17]. Summarizing these results, one can say that TMIs are most generally more stable when coordinated to four framework oxygens, though a twofold coordination (Cu(I) in ZSM-5, Cu(II) in FAU) should not be neglected. The deformed fourfold coordination with three short and one long TMI-zeolite oxygen bonds can be related to the presence of two (or more) Al neighbors, depending on the lo-

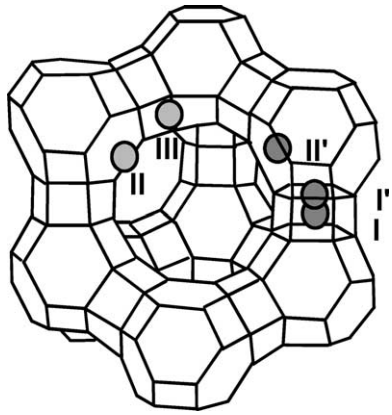

Fig. 1. Representation of the locations of extra framework cationic sites in faujasite; dark gray sites in sodalites, light gray sites in supercages.

cal structure [10,11,15,21,22]. Moreover, the comparison of EPR properties calculated for models of Cu(II)–FAU with Cu at sites II and III (Fig. 1) with experimental data indicates that the presence of several EPR signals is most probably related to Cu(II) sites with different coordinations [15]. It is well recognized that cations in FAU are mainly located in a few well-defined sites, namely I, I′, II, II′, and III. Sites II and III are located in the supercages, on top of a six-membered ring for the former, and near a four-membered ring for the latter.

3.2. The molecular aspect of TMI-zeolites

The "molecular" character of the TMI framework interaction is provided by the mixed contribution of metal (3d, 4s, 4p) and framework oxygen (2s, 2p) orbitals to bonding MOs, calculated for various TMI models [23–25]. The delocalization of these MOs involves an electron density distribution in the system which is quite different from that obtained for alkali-zeolite models, with MOs characteristic either of framework atom or alkali orbitals. The topological localization/delocalization of the electron density in a system can be evaluated using approaches such as electron localization functions [26], the atoms in molecules theory [27], or population analyses. The last methods are less precise and more sensitive to the methodology, but they are much more widely reported in the literature. Comparison of Mulliken atomic charges for various cluster models of Cu–ZSM-5, Cu–FAU, Zn–ZSM-5, etc. leads to the conclusion (even if only qualitative) that the TMI orbitals in these systems contain more electronic charge than they would in isolated TMIs [13,21, 23,24,28–31]. This effect, which originates in the quantum mechanical treatment of the models, and not in any arbitrary decomposition scheme, will be called "charge transfer" for simplicity.

This charge transfer amounts to 0.2–0.5 electron for Cu(I) models, depending on the representation of the second shell of neighbors (H or Si/Al). A detailed analysis of Cu(II)– and Fe(II)–FAU and –BEA models with various sizes has shown that the charge transfer amounts to approximately one electron and is little sensitive on cluster size [13,24]. Cu(II) with preferred fourfold coordination incorporates the transferred charge partly in its 3d hole and partly into the 4s, 4p orbitals. The singly occupied MO (SOMO) of this doublet system is delocalized on Cu3d and zeolite O2p orbitals, whereas the lowest unoccupied MO (LUMO), very close in energy, is of the same nature. The next unoccupied MO corresponds, as for all zeolite models (with protons and alkalis), to empty s counterion orbitals. The redox properties of the couple TMI(I)/TMI(II) in zeolite can then be related to the delocalization of the close SOMO and LUMO onto the full metal-framework system.

Moreover, it is noteworthy that the amount of charge distributed into the framework and "transferred" to the metal cation are not dependent on the relative Al positions, as it has been shown for Cu(II)–FAU [24] and Zn(II)–ZSM-5 models [21]. This result brings more reality to the concept of "molecularity": different random Al distributions in the framework can then lead to comparable TMI-zeolite electronic properties for different samples.

Finally, comparison between experimental and calculated EPR hyperfine coupling constants confirms the large delocalization of electron density on the metal and framework atoms, with an estimate of around 0.5 unpaired electron on the Cu ions [15].

3.3. The zeolite framework acts as a reservoir of charge: a supermolecular effect

Molecules adsorbed on TMIs are additional ligands with orbitals participating into the MOs of the complete system, in contrast with molecules adsorbed on alkali metal cations [10,24,25]. The binding energies of these adsorbates are generally decreased with respect to isolated metal cations [10,24,31]. However, specific sites may favor the adsorption, due to proper positions of the zeolite oxygens with respect to the metal, as it has been shown for NO or NO_2 on ZSM-5 models [10,23].

The evaluation of atomic charges is also useful in gaining a qualitative description of the variations encountered by the electron distribution upon addition or release of ligands. In this comparison, the errors inherent to every methodology used for distributing the electronic charge to specific atoms are compensated. They lead, for example, to comparable results between Bader-type and Mulliken analyses, although the first method leads to slightly more positive TMIs (around 0.1 a.u. for Cu(II)) than those of the second method. Moreover, maps of electron density differences can be used to confirm the conclusions drawn from these population analyses.

Keeping this in mind, it is interesting to compare the electron repartition between the zeolite framework and the metal cation without and with adsorbates. The Mulliken net charges reported for Cu(I)–ZSM-5 and Cu(II)–FAU models, including different adsorbates, are presented in Table 1.

Table 1
Mulliken net charges calculated on Cu, framework, and ligands (total charge) for Cu–ZSM-5 [13,14] and Cu–FAU models [18]

Ligand	Net charge		
	Cu(I)	ZSM-5	Ligand
	0.77	−0.77	
NO[a]	0.82	−0.67	−0.15
NO_2[a]	0.83	−0.58	−0.25
	0.57	−0.57	
NO_2[b]	0.67	−0.31	−0.26
	Cu(II)	FAU	Ligand
	0.72	−0.72	
$2H_2O$[c]	0.75	−1.01	0.26
$2NH_3$[c]	0.74	−1.11	0.37

[a] Ref. [13].
[b] Ref. [14].
[c] Ref. [18].

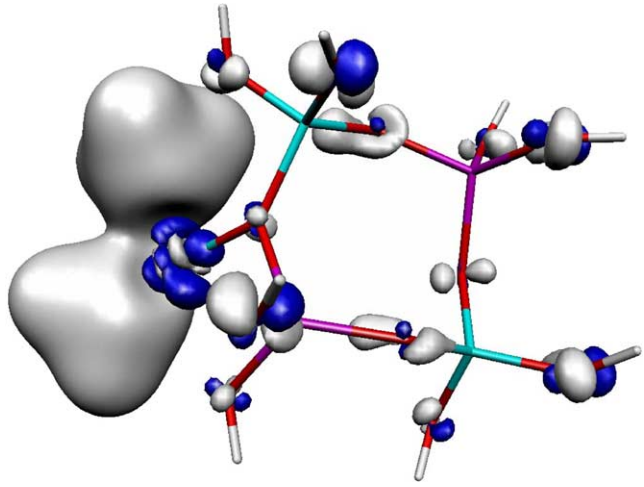

Fig. 2. Map of electron density difference between $(NH_3)_2$Cu(II)–FAU and Cu(II)–FAU models; blue: decrease of density; gray: increase of density.

In Cu(I)–ZSM-5 models, the zeolite-to-metal-charge transfer varies with the model chosen, but the response of both models to adsorption of electron acceptor molecules is similar: the charge transferred to NO or NO_2 originates mainly from the framework. At the opposite, when donor molecules are adsorbed, the positive net charge on the metal does not change very much, whereas the zeolite framework becomes more negative. This effect is illustrated in Fig. 2, which displays the difference of the total electron densities between $(NH_3)_2$Cu–FAU and Cu–FAU, showing that NH_3 binding is associated with more density distributed onto the oxygens of the framework. These results indicate that the framework plays the role of a reservoir of electronic charge, receiving or donating charge upon adsorption/desorption, this process being allowed by the MOs' delocalization.

It is worth noting that, upon ligand adsorption in Cu(II)–FAU, the nature of the SOMO changes with an increased metal character in addition to additional ligand contributions, leading to an increased spin density on the metal. This result is in agreement with experimental observations of EPR signals appearing upon water addition [32].

These examples show that there is a strong interchange of electron density between the framework and the TMIs, leading to a supermolecular picture of the full system. It is worth noting that this aspect of the exchange of electron density between the zeolite framework, the TMIs, and the adsorbates, is lost if the model chosen to represent the zeolite framework is too crude, for example, limited to $Al(OH)_4^-$ [29] or represented with water molecules [23,31].

4. The reduction of nitrogen oxides using TMI-zeolite: an example of reactivity

4.1. *DeNO$_x$ on TMI-zeolite*: *active center and mechanism*

Several mechanisms have been proposed [2–8], but a common feature of NO_x and N_2O transformation into N_2 on TMI-zeolite is the involvement of the redox couple $TM^{n+}/TM^{(n+1)+}$ in the catalytic cycle. This seems true whatever the reaction, catalytic decomposition, or catalytic reduction, and whatever the reductant, NH_3, CO, and even hydrocarbons, as illustrated in Fig. 3 for the SCR of NO and N_2O on Cu- and Fe-zeolite, respectively. Some interesting features of TMI-zeolite catalysts for these reactions will be illustrated for the SCR of NO by NH_3 on Cu–FAU.

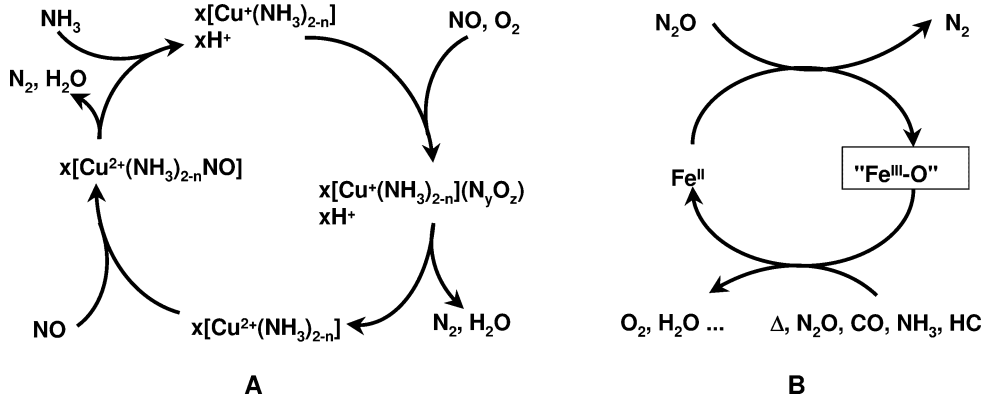

Fig. 3. (A) Catalytic cycle of the SCR of NO by NH_3 on Cu–FAU. (B) Catalytic cycle of the N_2O reduction on Fe-zeolite.

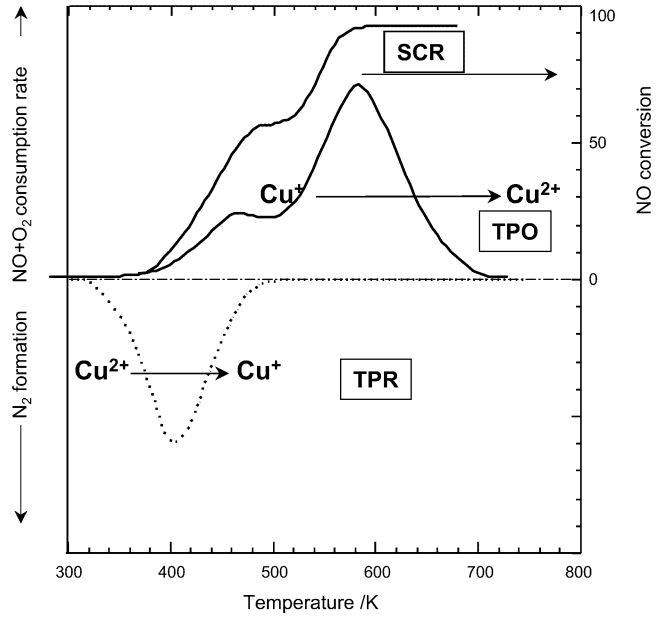

Fig. 4. TPR, TPO, and SCR profiles on Cu(76)–FAU. Conditions: VVH = 250,000 h^{-1}, ramp = 5 K min^{-1}; TPR of Cu(II)–FAU, $NO/NH_3/He$ = 0.2/0.2/99.6; TPO of Cu(I)–FAU, $NO/O_2/He$ = 0.2/3.0/96.8; SCR, $NO/NH_3/O_2/He$ = 0.2/0.2/3.0/96.6.

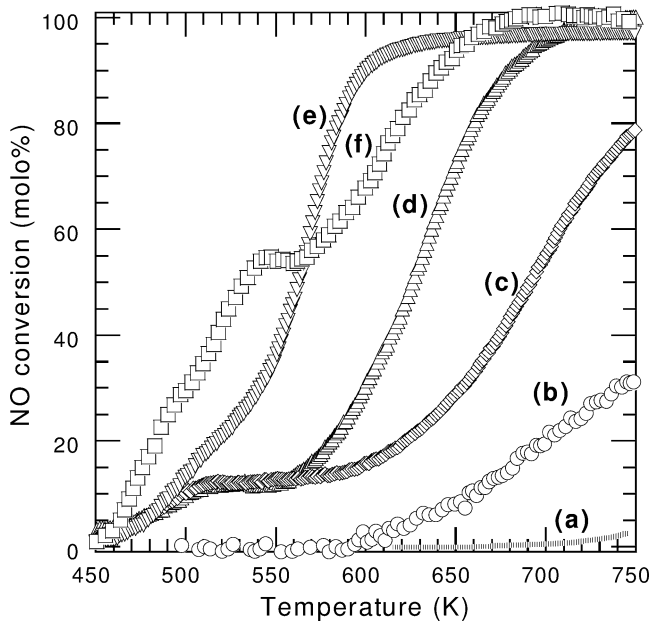

Fig. 5. SCR of NO by NH_3 as a function of temperature on CuHNa–FAU, (a) Na–FAU, (b) H–FAU, (c) Cu(25)H(0)Na–FAU, (d) Cu(26)H(26)Na–FAU, (e) Cu(28)H(51)Na–FAU, (f) Cu(27)H(71)–FAU; conditions: $NO/NH_3/O_2/He$ = 0.2/0.2/3/96.6; ramp = 10 K min^{-1}, space velocity = 250,000 h^{-1}.

The SCR of NO by NH_3 on Cu-zeolite is regulated by a redox cycle of copper ions [33–36], in which oxidation is the rate determining step. Strong support of this assumption is provided by TPR/TPO experiments with NO + NH_3 and NO + O_2 [36], respectively, which are shown in Fig. 4. Cu(II)–FAU is reduced by NO + NH_3 to Cu(I)H–FAU, which in turn is oxidized to Cu(II)–FAU by NO + O_2. The main peak of Cu(I)–FAU oxidation occurs 200 K above the reduction peak. The unique feature of the process demonstrated by TPO and SCR with $^{15}NH_3$ concerns the oxidation of Cu^+ complexes, which is faster by NO + O_2 than by O_2 alone [36]. The occurrence of two peaks in the TPO profile is due to the oxidation of Cu(I) species siting in supercages (oxidation peak at 480 K), and in sodalite (oxidation peak at 600 K). It is worth noting that the two oxidation peaks in the TPO profiles and the two waves of NO conversion in the SCR merely take place at the same temperatures.

The facile reduction of Cu(II)–FAU could be related with the molecular aspect of the TMI-zeolite system, as pictured by the QM calculations (vide supra). It was indeed found that the electronic state of Cu in Cu(II)–FAU and Cu(I)H–FAU models were comparable, whereas the delocalization of the MOs among metal and framework was different [24].

4.2. $DeNO_x$ on TMI-zeolite: factors influencing the reactivity

The oxidation step determines the SCR rate which depends on the number of active Cu(I) centers and their oxidability. The SCR was studied on Cu–FAU of various Cu contents (2.9 < Cu < 7.9 wt%), which correspond to theoretical exchange degrees in Cu^{2+} from 25 to 76%. The TOF (number of NO molecules transformed per Cu atom) was calculated at 500 K, with VVH = 250,000 h^{-1} and $NO/NH_3/O_2/He$ = 0.2/0.2/3.0/96.6 [36]. A sixfold increase of TOF occurs upon the threefold increase of Cu content. A similar behavior was reported by Komatsu et al. [37] for the SCR on Cu–MOR catalysts. In view of the correlation between copper content and SCR specific activity, we proposed that the active sites below 550 K are composed of Cu ions in close vicinity, possibly $[CuOCu]^{2+}$, stabilized by NH_3 and located in the supercages. Above 600 K, all Cu ions become active. Komatsu et al. [37] also proposed $[CuOCu]^{2+}$ as active species with a nitrate-like species as intermediate. One can anticipate that the proportion of such species, or next nearest neighbor Cu ions, should increase with increasing Cu content if Cu ions are located randomly at the cation sites. The occurrence of $[CuOCu]^{2+}$ species in the supercages was never observed, and a unique possibility would be two Cu^{2+} ions located at sites II and III (Fig. 1). Site III can only be populated by cations at high exchange degree and low Si/Al ratios.

There is little effect of the Cu content on its oxidability. Whatever the amount of Cu, the main peak of Cu^+ oxidation by NO + O_2 appears at 570–580 K [36]. In contrast, siting influences greatly the reactivity of the Cu species. This is particularly true for zeolites containing small cavities, e.g., FAU and EMT. Access of reactants to active sites located within these cavities is strongly hindered. However, a preliminary exchange of Na–FAU with, e.g., Ca, Ba, La, followed by a calcination, impedes the access of Cu to these cavities [38]. The catalytic materials thus elaborated exhibit

higher reactivity and better selectivity in the SCR of NO_x by NH_3 [39], even at low Cu content.

4.3. *DeNO$_x$ on CuH–FAU: the influence of protons*

A remarkable feature is the effect of protons on the reactivity of Cu species. Fig. 5 shows the SCR of NO by NH_3 on CuHNa–FAU with the same Cu content (~ 2.8 wt%) but with various proton amounts [40]. It is worth noting that whatever the sample the selectivity to N_2 was close to 100% in the range of temperature investigated, and that both Na–FAU and H–FAU exhibit low activity. In contrast, CuHNa–FAU catalysts are active and the rate increases with the proton content in the sample. The light-off temperature (at 50% NO conversion) thus decreases from 690 to 535 K moving from Cu(25)H(0)Na–FAU to Cu(27)H(71)Na–FAU. This clear incidence of protons on the catalytic properties of Cu–FAU could be accounted for:

1. By a modification of the redox properties of Cu^+/Cu^{2+}, which are involved in the catalytic cycle.
2. By a change of accessibility to Cu sites in Cu–FAU.
3. By a direct involvement of protons in the catalytic transformation for NO. For instance, the need for a good balance between Brønsted and Fe sites in a cooperative mechanism was proposed in the SCR on Fe–MFI [41].
4. By a higher stabilization of dinuclear Cu clusters by protons than by Na, owing to a stronger interaction with NH_3.

Better insight into the role of protons for promoting the SCR of NO has been accessed through H_2–TPR, NO + O_2–TPO and adsorption/desorption of CO and NH_3 [40].

In H_2–TPR, the reduction step $Cu^{2+} \rightarrow Cu^+$ in Cu–FAU takes place between 450 and 800 K and is composed of two events. These events were assigned to the reduction of Cu^{2+} species in different lattice positions of FAU: located in supercage and sodalite cavities, respectively. The proportion of Cu^{2+} in supercages which is ca. 30% in Cu(25)H(0)Na–FAU decreased upon exchanging Na^+ for H^+. It is worth noting that the temperature of maximum rate for Cu^{2+} reduction in sodalite remains more or less constant whatever the nature of cocation. There is thus very little effect of the proton content on Cu^{2+} reduction.

TPO experiments were carried out on Cu(I)HNa–FAU. The TPO profiles were shifted by ca. 100 K to lower temperatures when Na^+ was substituted for H^+ in Cu–FAU catalysts. One can conclude that H^+ as cocation makes the oxidation of Cu^+ to Cu^{2+} easier as compared to Na^+. Insofar as the reoxidation of Cu^+ to Cu^{2+} has been proposed as the rate determining step in the SCR [36], an easier oxidability of Cu^+ in Cu(27)H(71)Na–FAU would explain the faster SCR rate observed on this sample (Fig. 5).

To sum up, the TPR and TPO experiments have provided evidence of changes in the Cu^+/Cu^{2+} redox cycle, which could explain in part the behavior of samples in the SCR. These changes of redox properties, and especially that of Cu^+ to Cu^{2+} oxidation (rate determining step), could be related to a modification of the electronic properties of Cu^+ depending on the nature of cocations, H^+ or Na^+ [40].

The accessibility to Cu centers has been probed from chemisorption of CO followed by TPD and DRIFT experiments [40]. Upon substituting Na^+ for H^+, on the one hand CO desorbs at higher temperature, and on the other hand the CO uptake increases. In the C–O stretching region of adsorbed CO (2200–2100 cm^{-1}), two main bands were observed after adsorption at 298 K of CO/Ar (1/99), at 2160 and 2140 cm^{-1}. These bands maintain after evacuation in Ar at the same temperature, and were unambiguously assigned to CO adsorbed on Cu^+ species located in the supercages. These species are thermally stable since full desorption occurs at above 420–450 K. Palomino et al. [42] and Borovkov and Karge [43] concluded that CO–Cu^+ at site II is responsible for the band at ca. 2160 cm^{-1}. The absorption at ca. 2140 cm^{-1} has been assigned to CO–Cu^+ adducts at sites II^* [42]. Site II^*, not included in the conventional nomenclature, is located at the center of six-membered rings connecting sodalite cages with supercages (Fig. 1). Such a position could be reached by Cu^+ siting at sites II′ and attracted toward sites II^* by the withdrawal power of CO ligand. From IR [43–45] and in situ XRD [42] studies, it was indeed concluded that a migration of Cu^+ ions from sites in sodalite cages to supercages definitely occurs upon CO exposure. Moreover, it was found on CuNa–FAU that a significant fraction of Cu^+ did not migrate to the supercages and maintained located at sites I or I′ even at high CO pressure [43]. This is likely due to the presence of Na at site II′.

Regarding this last point, the uptake of CO per Cu site, which represents the accessibility to Cu species, is of 0.90 on Cu(27)H(71)Na–FAU and steadily decreases upon substitution of H^+ for Na^+ to reach 0.34 on Cu(25)H(0)Na–FAU. In agreement with the occupation by Cu^+ of hidden sites for CO access in CuNa–FAU, one can speculate that substituting Na^+ for H^+ makes the migration of Cu^+ from sodalite cages to supercages easier. This behavior could also explain the higher SCR reactivity of Cu(27)H(71)Na–FAU since NH_3 and H_2O are ligands of stronger attracting power than CO. The less hindered migration of Cu from sodalite to supercages, in the presence of protons, may actually account for a higher proportion of dinuclear Cu active species within the supercage. Such an effect would then correspond to a proton-promoted stabilization of dinuclear Cu species.

The direct involvement of protons in the deNO$_x$ process has been probed from NH_3–TPD experiments on CuHNa–FAU [40]. It was concluded that 3.3–3.4 NH_3 ligands were adsorbed per Cu on CuHNa–FAU with high proton content, but only 1.9 at low proton content. The value of ca. 3 NH_3 per Cu site is in good agreement with that reported on Cu–FAU with high exchange degree [36,46]. Actually, the lower values of ca. 1.9 for NH_3/Cu found on CuHNa–FAU with high Na content could be put in parallel with the lowest CO/Cu values found in CO–TPD on the same samples

(vide supra). As for CO–TPD experiments, the lowest NH_3 uptake, averaged per Cu site, could be assigned to hidden Cu sites due to the presence of Na. The two most active samples, i.e., Cu(27)H(71)Na–FAU and Cu(26)H(51)Na–FAU, retain in their range of light-off temperature (520–600 K) equilibrated amounts of NH_3 on both H^+ and Cu sites. One could therefore also conclude that their highest activity in SCR might result from a dual site mechanism occurring on redox and Brønsted sites as proposed by Long and Yang [41] for Fe–ZSM-5 and Topsøe et al. [47] for V_2O_5–WO_3/TiO_2 catalysts.

These series of experiments have shown that none of the proposed hypotheses for explaining the behavior of CuHNa–FAU as a function of H and Na contents can be ruled out. One of those deals with the redox properties of Cu, and more specifically with the oxidation of Cu^+ to Cu^{2+}, which are correlated with their electronic properties. Quantum chemical calculations have provided additional information on this last point. The decrease of temperature of Cu(I) oxidation to Cu(II) cannot be assigned to a higher amount of dinuclear Cu species, since in CuNa–FAU of various Cu contents, the oxidation temperature of Cu(I) remained the same [36]. This behavior is specifically related to the change of redox properties of Cu in the presence of protons. Considering the supermolecular aspect of TMI-zeolite, the electronic properties of model clusters CuHNa–FAU have been thus investigated by quantum chemical calculations.

For the QM calculations [40], the Cu(I)H–FAU zeolite, obtained by reduction of Cu(II)–FAU, has been modeled with one six-membered ring containing Cu^+, associated with the neighboring four-membered ring, in order to accommodate enough Al/cation couples (4 Al centers). The clusters studied, Na_3Cu, H_3Cu and three Na_2HCu, models of CuHNa–FAU, are illustrated in Fig. 6.

Since the presence of protons favors the oxidation of the system, one would expect the first ionization energy (EI) to be smaller for H_3Cu than for Na_3Cu, the HOMO being characteristic of Cu3d and zeolite O2p orbitals. In fact, the calculated EIs show the opposite trend, with 7.0 and 6.0 eV for H_3Cu and Na_3Cu, respectively, with intermediate values for Na_2HCu. This order is reversed when the electron affinities (EA) are compared and using the DFT-based concept of hardness $\chi = \delta^2 E/\delta N^2 \# \frac{1}{2}(\text{EI–EA})$. One concludes that the hardness of the fully protonated model (2.9 eV) is much larger than that of Na_3Cu (2.07 eV), with intermediate values (2.2–2.4 eV) for the three Na_2HCu models. This leads us to expect a weaker global hardness for a system with a majority of Na cations and few protons than for a fully protonated system. Hardness being related to acidity in zeolites [48], these results indicate that the protons in H_3Cu are more acidic than those in Na_2HCu, which has been confirmed by the calculation of their proton affinities (smaller in the fully protonated model) [40]. That indicates a weakly bonded proton, which is thereby more available in the reaction of Cu(I) oxidation: $2\text{Cu(I)H–FAU} + \frac{1}{2}O_2 \rightarrow 2\text{Cu(II)} + H_2O$.

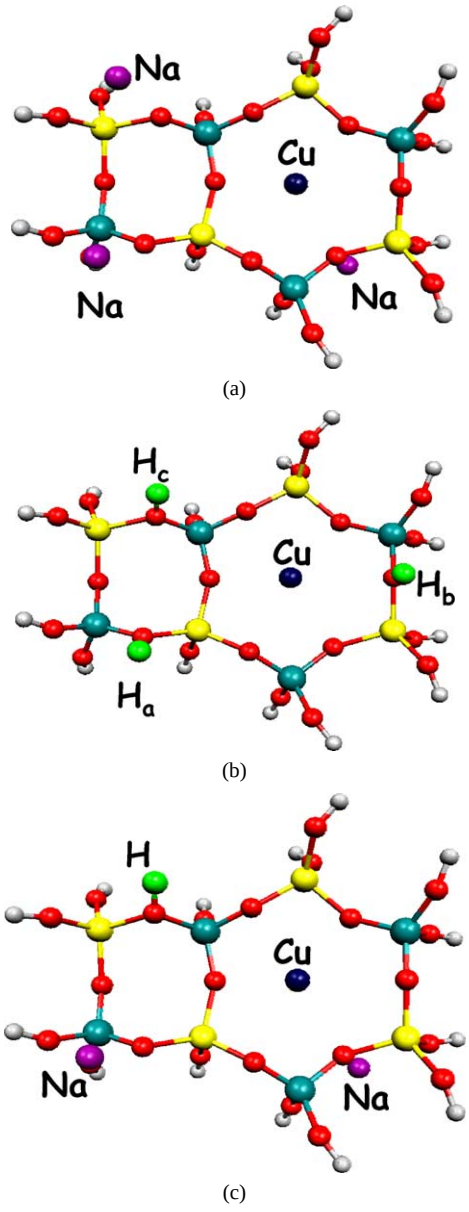

Fig. 6. Model clusters Na_3Cu (a), H_3Cu (b), and Na_2HCu (c); Si (yellow), Al (blue), O (red), Cu (black), H (white), and Na (purple).

The analysis of the electronic structures of the models studied above brings more insight into the description of the so-called supermolecular aspect of zeolites:

1. The upper occupied MOs of the two extreme cases, i.e., H_3Cu and Na_3Cu, show an obvious delocalization of several occupied MOs onto Cu and the zeolite oxygens for H_3Cu, whereas it is not the case for Na_3Cu;
2. The charge transfer from the framework to the four cations is much larger for H_3Cu (due to the covalency of the OH bonds), which means a less negative framework (0.7 electron less than for Na_3Cu).

These results indicate that the metal-framework bonding differs according to the nature of the other cations. The catalytic behavior of the zeolite is thus dependent on all the

elements which constitute this system and which are, in fact, strongly cross-dependent.

5. Concluding remarks

In the past decade, modeling properties of zeolite catalysts with QM or QM/MM methods has continuously developed, thanks to the increase of computing power. The access to QM of models with large realistic size becomes then a real and exciting possibility. This is essential for reproducing the structural and electronic properties of TMI-zeolite with accuracy. The first attempts in this area have been to reach a better knowledge of the material itself, i.e., location of the TMI sites with respect to the various frameworks, description of the metal cations, isolated species or more complex oxocations, coordination with the aluminosilicate framework, and, with the aim of a validation of the modeling, prediction of spectroscopic properties, such as electronic absorption spectra or magnetic electron spin properties.

From all these studies, we have gained a picture of the material which looks like that of a large organometallic system, with a zeolite framework being a multidentate ligand interacting strongly with the dispersed TMIs. This description of TMI-zeolites is not completely unexpected for coordination chemists, but it may appear very "molecular" for scientists in materials, who are more familiar with periodic model systems. TMI-zeolites are nonperiodic solids, because of the nonperiodic distribution of Al and TMIs. Moreover, the nonpolarity of these solids forbids translational symmetry. The description we get from modeling, i.e., a complex ligand (including also other cations than TMIs) interacting strongly with its TM cations, allows us to understand better the global properties of the solid, whatever the local variations of composition and structure could be.

The studies involving the interaction of the zeolite catalysts with reactants have also brought much understanding of how they work together. This is the first step for a detailed description of reaction mechanisms. In this first step, the analyses of the electron density changes upon adsorption/desorption of donor or acceptor ligands have underscored the supermolecular aspect of the whole system, where the TMI-zeolite response to the various ligands shows a large ability to accommodate all electronic effects.

Dissecting the physics behind the simulated properties is thus an important issue in modeling studies. In the near future, detailed studies of reaction mechanisms involving transition states and intermediates will certainly develop. The state of art at present will help in designing adequate models for TMI active sites, which must be able to mimic the very large geometric and electronic adaptability of these catalysts.

In confronting both theoretical studies and spectroscopic data, anticipated breakthroughs will be now the identification of reaction mechanisms, nature of active centers, and their dependency upon the local environment. The reduction of nitrogen oxides using TMI-zeolite catalysts is an archetypal example of such an achievement, due to the crucial importance of the process and the high reactivity of these materials. Specifically, the experiments in NO_x reduction by NH_3 on Cu–FAU demonstrated that the oxidation of Cu(I) to Cu(II) is the limiting step. The modeling of Cu(I)HNa–FAU has shown that the proton ability would be the key factor in the reoxidation step, with the need for a good balance between the active centers, Cu, and the protons for the H-promoted reoxidation of these active centers. From this challenging achievement, the rational design of new nanostructured TMI-zeolite may be expected.

Acknowledgment

The authors thank all their colleagues from the laboratory who participated in these studies about TMI-zeolite.

References

[1] P. Gry, in: Proceedings of NOXCONF'2001, ADEME Publication, Paris, 2001, Session 8.
[2] H. Bosch, F. Janssen, Catal. Today 2 (1988) 369.
[3] M. Iwamoto, in: M. Misono, Y. Moro-oka, S. Kimura (Eds.), Future Opportunities in Catalytic and Separation Technologies, Elsevier, Amsterdam, 1990, p. 121.
[4] A. Fritz, V. Pitchon, Appl. Catal. B 13 (1997) 1.
[5] V.I. Pârvulescu, P. Grange, B. Delmon, Catal. Today 46 (1998) 233.
[6] Y. Traa, B. Burger, J. Weitkamp, Micropor. Mesopor. Mater. 30 (1999) 3.
[7] F. Kapteijn, J. Rodriguez-Mirasol, J.A. Moulijn, Appl. Catal. B 9 (1996) 25.
[8] G. Delahay, D. Berthomieu, A. Goursot, B. Coq, in: M. Keane (Ed.), Interfacial Applications of Environmental Engineering, Dekker, New York, in press.
[9] A.T. Bell, in: G. Centi, B. Wichterlova, A.T. Bell (Eds.), Catalysis by Unique Metal Ion Structures in Solid Matrices, Kluwer Academic, Dordrecht, 2001, p. 55.
[10] J. Sauer, D. Nachtigallova, P. Nachtigall, in: G. Centi, B. Wichterlova, A.T. Bell (Eds.), Catalysis by Unique Metal Ion Structures in Solid Matrices, Kluwer Academic, Dordrecht, 2001, p. 221.
[11] D. Nachtigallova, P. Nachtigall, J. Sauer, Phys. Chem. Chem. Phys. 3 (2001) 1552.
[12] L.A.M.M. Barbosa, R.A. Van Santen, J. Hafner, J. Amer. Chem. Soc. 128 (2001) 4530.
[13] D. Berthomieu, A. Goursot, J.-M. Ducéré, G. Delahay, B. Coq, A. Martinez, in: A. Galarneau, F. Di Renzo, F. Fajula, J. Vedrine (Eds.), Zeolites and Mesoporous Materials at the Dawn of the 21st Century, Elsevier, Amsterdam, 2001, p. 15-P-23.
[14] A. Delabie, K. Pierloot, M.H. Groothaert, B.M. Veckhuysen, R.A. Schoonheydt, Micropor. Mesopor. Mater. 37 (1998) 209.
[15] D. Berthomieu, J.-M. Ducéré, A. Goursot, J. Phys. Chem. B, in press.
[16] P. Nachtigall, D. Nachtigallova, J. Sauer, J. Chem. Phys. B 104 (2000) 1738.
[17] B. Wichterlova, D.J. Dedecek, Z. Sobalik, in: G. Centi, B. Wichterlova, A. Bell (Eds.), Catalysis by Unique Metal Ion Structures in Solid Matrices, Kluwer Academic, Doordrecht, 2001, p. 31.
[18] L. Drozdova, R. Prins, D.J. Dedecek, Z. Sobalik, B. Wichterlova, J. Phys. Chem. B 106 (2002) 2240.
[19] Z. Sobalik, Z. Tvaružkova, B. Wichterlova, J. Phys. Chem. B 102 (1998) 1077.

[20] R.A. van Santen, D.L. Vogel, Adv. Solid State Chem. 1 (1989) 151.
[21] A.L. Yakolev, A.A. Shubin, G.M. Zhidomirov, R.A. van Santen, Catal. Lett. 70 (2000) 175.
[22] K. Pierloot, A. Delabie, M.H. Groothaert, R.A. Schoonheydt, Phys. Chem. Chem. Phys. 3 (2001) 2174.
[23] L. Rodriguez-Santiago, M. Sierka, V. Branchadell, M. Sodupe, J. Sauer, J. Am. Chem. Soc. 120 (1998) 1545.
[24] D. Berthomieu, S. Krishnamurty, B. Coq, G. Delahay, A. Goursot, J. Phys. Chem. B 105 (2001) 1149.
[25] A. Delabie, C. Vinckier, M. Flock, K. Pierloot, J. Phys. Chem. A 105 (2001) 5479.
[26] A.D. Becke, K.E. Edgecombe, J. Chem. Phys. 92 (1990) 5397.
[27] R.F.W. Bader, Atoms in Molecules—A Quantum Theory, Oxford Univ. Press, Oxford, 1990.
[28] W.F. Schneider, K.C.H.R. Ramprasad, J.B. Adams, J. Phys. Chem. B 101 (1997) 4353.
[29] W.F. Schneider, K.C.H.R. Ramprasad, J.B. Adams, J. Phys. Chem. B 102 (1998) 3705.
[30] B.L. Trout, A.K. Chakraborty, A.T. Bell, J. Phys. Chem. 100 (1996) 17582.
[31] W.F. Schneider, R.K.C. Hass, K.C.H.R. Ramprasad, J.B. Adams, J. Phys. Chem. 100 (1996) 6032.
[32] G. Turnes Palomino, P. Fisicaro, S. Bordiga, A. Zecchina, E. Giamello, C. Lamberti, J. Phys. Chem. B 104 (2000) 4064.
[33] W.B. Williamson, J.H. Lunsford, J. Phys. Chem. 80 (1976) 2664.
[34] M. Mitzumoto, N. Yamazoe, T. Seiyama, J. Catal. 55 (1978) 119.
[35] S.W. Ham, H. Choi, I.S. Nam, Y.G. Kim, Catal. Lett. 42 (1996) 35.
[36] S. Kieger, G. Delahay, B. Coq, B. Neveu, J. Catal. 183 (1999) 267.
[37] T. Komatsu, M. Nunokawa, I.S. Moon, T. Takahara, S. Namba, T. Yashima, J. Catal. 148 (1994) 427.
[38] S. Kieger, G. Delahay, B. Coq, Appl. Catal. B 25 (2000) 1.
[39] B. Coq, G. Delahay, F. Fajula, S. Kieger, B. Neveu, US Patent 6.221.324, 2001.
[40] G. Delahay, E. Ayala Villagomez, J.M. Ducéré, D. Berthomieu, A. Goursot, B. Coq, Chem. Phys. Chem., in press.
[41] R.Q. Long, R.T. Yang, J. Catal. 188 (1999) 332.
[42] G. Turnes Palomino, S. Bordiga, A. Zecchina, G.L. Marra, C. Lamberti, J. Phys. Chem. B 104 (2000) 8641.
[43] V.Yu. Borovkov, H.G. Karge, J. Chem. Soc. Faraday Trans. 191 (1995) 2035.
[44] Y.-Y. Huang, J. Catal. 30 (1973) 187.
[45] J. Howard, J.M. Nicol, Zeolites 8 (1988) 142.
[46] Y.-Y. Huang, E.F. Vansant, J. Phys. Chem. 77 (1973) 663.
[47] N.-Y. Topsøe, J.A. Dumesic, H. Topsøe, J. Catal. 151 (1995) 241.
[48] A. Corma, in: H. Beyer, H.G. Karge, I. Kiricsi, J.-B. Nagy (Eds.), Catalysis by Microporous Materials, Elsevier, Amsterdam, 1995, p. 736.